Self-Consistent-Field Theory of Viscoelastic Behavior of Inhomogeneous Dense Polymer Systems

Tetsufumi Shima,[†] Hirokazu Kuni,[‡] Yutaka Okabe,[§] Masao Doi,[⊥] Xue-Feng Yuan,[#] and Toshihiro Kawakatsu*,[×]

Nippon Ericsson K.K., Ichibankan 5F, YRP Center, 3-4 Hikarino-oka, Yokosuka, Kanagawa 239-0847, Japan; Dev. INS No.6, Financial Solution Center #2, IBM Japan, Ltd., Tokyo 103-8510, Japan; Department of Physics, Tokyo Metropolitan University, Tokyo 192-0397, Japan; Department of Computational Science and Engineering, Nagoya University, Nagoya 464-8603, Japan; Department of Mechanical Engineering, Kings College London, Strand, London WC2R 2LS, United Kingdom; and Department of Physics, Tohoku University, Sendai 980-8578, Japan

Received April 2, 2002; Revised Manuscript Received August 29, 2003

ABSTRACT: By combining the self-consistent-field (SCF) model and a reptation model, we propose a unified molecular model to explicitly account for dynamics of chain conformation in studying fast polymeric fluid flows in which the polymer chains can be severely stretched and the fluid can even become inhomogeneous. In the governing equations of the unified model, we directly couple the probability distribution function $P(\mathbf{u};s,\mathbf{r})$ of the tangent vector $\mathbf{u} \equiv d\mathbf{R}(s)/ds$ at the sth segment at position $\mathbf{r}$, with the statistical weight, $Q(s,\mathbf{r};s',\mathbf{r}')$, of the subchain between sth and s'th segments at the positions of $\mathbf{r}$ and $\mathbf{r}'$, respectively. The polymeric stress responses under flow condition can be readily calculated from the second moment of $P(\mathbf{u};s,\mathbf{r})$, $\mathbf{A}(s,\mathbf{r}) \equiv \langle \mathbf{uu} \rangle \equiv \int \mathbf{uu} P(\mathbf{u};s,\mathbf{r})\, d\mathbf{u}$. The model was first validated in homogeneous simple shear flow. The quantitative agreements between the polymeric stresses evaluated by this novel method and the results of the reptation theory have been found. The model was then tested in a case study of grafted polymer melt brushes under strong shear flow. Our results demonstrate that the unified model provides a very promising way for modeling highly nonlinear polymer fluid flow, and it can also overcome the difficulty of the standard SCF technique when it is applied to highly nonequilibrium systems.

1. Introduction

Although viscoelasticity is one of the central issues of dynamics of dense polymers, it has mainly been studied for uniform systems.[1] There are, however, many examples of viscoelastic behavior in inhomogeneous systems. One example is the viscoelastic phase separation, where the conformation of polymer chain is deformed by an internal flow field that is caused by the inhomogeneity in the segment density distribution.[2] Another example is the slippage of polymer brushes grafted onto a solid surface.[3,4] When we impose a shear deformation on two parallel solid plates each of which is covered by a grafted polymer brush, the chains are strongly stretched due to entanglements, which leads to a modification of the friction between the plates. The essential point in these viscoelastic phenomena is the combination of the spatial inhomogeneity and the strongly stretched chain conformation. Traditionally, these two characters have been theoretically treated rather separately. The inhomogeneous structure can be quantitatively analyzed with the self-consistent-field (SCF) technique,[5,6] which accounts for the conformational entropy of the polymer chains explicitly. On the other hand, the dynamics of strongly stretched chains that are mutually entangled has been well described by the reptation theory,[1] which approximates the entangled polymer chains by a single primitive chain confined in a tube. Although both of these theoretical treatments are successful, there have been very few theoretical works that intend to treat the spatial inhomogeneity and the dynamics of entangled polymers simultaneously. Most of the existing dynamical extensions of the SCF method[7−12] are essentially based on the local equilibrium assumption of the chain conformation under the given segment density distributions. However, such an assumption cannot be justified for strongly stretched chains, for which the segment density distributions are not enough to specify the state of the system.

In this article, we propose a complete description of our new SCF technique[13,14] that can be applied to inhomogeneous polymer systems where chains are strongly stretched. Our model is a combination of the SCF technique and the reptation theory, where the anisotropy in the distribution of the tangent vectors is taken into account. Such a use of the tangent vector distribution function is originally proposed by Maurits, Zvelindovsky, and Fraaije in their formulation of the dynamic SCF technique.[15] Very recently, some other groups started to use similar techniques.[16,17] Fredrickson combined the two fluid model and the SCF technique to simulate the dynamics of polymer solutions.[16] Milhailovic, Lo, and Shnidman extended the SCF theory by combining it with the dumbbell model that accounts for the Rouse dynamics.[17] While these dynamic SCF theories by the other groups are aimed to model dilute polymer solutions and mixtures, the present theory is for modeling dense polymer mixtures where the entanglement effect is very important.

* To whom correspondence should be addressed.
[†] Nippon Ericsson K.K.
[‡] IBM Japan, Ltd.
[§] Tokyo Metropolitan University.
[⊥] Nagoya University.
[#] Kings College London.
[×] Tohoku University.

10.1021/ma0205257 CCC: $25.00
Published on Web 11/07/2003

2. Model

Let us consider a melt of a linear homopolymer composed of N segments of size a. For simplicity, we assume that this segment size a is equal to the tube diameter that characterizes the reptation theory.[1] Note that the tube diameter is usually much larger than the persistent length of polymer chain. We use a continuum description of the chain by introducing an index s ($0 \le s \le N$) to specify each segment and denote the position of the sth segment as $\mathbf{R}(s)$. Then, the chain conformation is characterized by two probability distribution functions. One is the probability distribution function $P(\mathbf{u};s,\mathbf{r})$ of the tangent vector $\mathbf{u} \equiv d\mathbf{R}(s)/ds$ at the sth segment at position $\mathbf{r}$, and the other is $Q(s,\mathbf{r};s',\mathbf{r}')$ which is the statistical weight of the subchain between sth and s'th segments that are fixed at $\mathbf{r}$ and $\mathbf{r}'$, respectively.[1,5,6] This statistical weight $Q(s,\mathbf{r};s',\mathbf{r}')$ is also called "path integral" or "propagator" and accounts for the conformation of the course-grained chain.

As the tangent vector $\mathbf{u}$ connects adjacent segments, its probability distribution function $P(\mathbf{u};s,\mathbf{r})$ is related to the statistical weight $Q(s,\mathbf{r};s',\mathbf{r}')$. Such a relation is obtained by following the standard technique.[1,5] We adopt the mean-field approximation, where a tagged chain in a dense polymer solution is modeled as an ideal chain in an external potential field (mean field) $V(\mathbf{r})$ imposed by the other chains. Because of the self-consistency requirement described later, this external potential $V(\mathbf{r})$ is called the self-consistent field. Using the canonical ensemble of temperature T, the statistical weight of the conformation $Q(s,\mathbf{r};s',\mathbf{r}')$ is given by

$$Q(s',\mathbf{r}';s,\mathbf{r}) = \int \delta\{\mathbf{r}(s)\} \exp\left[-\frac{1}{k_B T}\{\int_{s'}^{s} V(\mathbf{r}(\mathbf{s}))\, ds\}\right] \quad (1)$$

where $\int \delta\{\mathbf{r}(s)\}$ means a sum over all possible chain conformations that are consistent with the probability distribution of the tangent vectors $P(\mathbf{u};s,\mathbf{r})$, and k_B is the Boltzmann constant. The ideal chain statistics of the chain conformation requires the following Chapman−Kolmogorov relation:

$$\begin{aligned} Q(s',\mathbf{r}';s+1,\mathbf{r}) &= \int d\mathbf{r}''\, Q(s',\mathbf{r}';s,\mathbf{r}'')\, Q(s,\mathbf{r}'';s+1,\mathbf{r}) \\ &= \int d\mathbf{r}''\, Q(s',\mathbf{r}';s,\mathbf{r}'') \times \\ &\qquad P(\mathbf{r}-\mathbf{r}'';s,\mathbf{r}) e^{-V(\mathbf{r})/k_B T} \end{aligned} \quad (2)$$

By assuming that the characteristic length scale of the spatial variation of the self-consistent field $V(\mathbf{r})$ is large enough compared to the segment size, we expand the right-hand side around $\mathbf{r}'' = \mathbf{r}$ and, retaining up to second order in $\mathbf{r}'' - \mathbf{r}$, then obtain

$$\begin{aligned} \frac{\partial}{\partial s} Q(s,\mathbf{r};s',\mathbf{r}') = \frac{1}{2}\nabla\nabla:\{\mathbf{A}(s,\mathbf{r})\, Q(s,\mathbf{r};s',\mathbf{r}')\} - \\ \nabla\cdot\{\bar{\mathbf{u}}(s,\mathbf{r})\, Q(s,\mathbf{r};s',\mathbf{r}')\} - \frac{1}{k_B T} V(\mathbf{r})\, Q(s,\mathbf{r};s',\mathbf{r}') \end{aligned} \quad (3)$$

where the vector $\bar{\mathbf{u}}(s,\mathbf{r}) = (\bar{u}_\mu(s,\mathbf{r}))$ and the tensor $\mathbf{A}(s,\mathbf{r}) = (A_{\mu\nu}(s,\mathbf{r}))$, where μ and ν indicate the Cartesian coordinates x, y, and z, are the first and second moments of $P(\mathbf{u};s,\mathbf{r})$ defined by

$$\bar{\mathbf{u}}(s,\mathbf{r}) \equiv \langle \mathbf{u} \rangle \equiv \int \mathbf{u} P(\mathbf{u};s,\mathbf{r})\, d\mathbf{u} \quad (4)$$

and

$$\mathbf{A}(s,\mathbf{r}) \equiv \langle \mathbf{u}\mathbf{u} \rangle \equiv \int \mathbf{u}\mathbf{u} P(\mathbf{u};s,\mathbf{r})\, d\mathbf{u} \quad (5)$$

and we also used the abbreviation

$$\nabla\nabla:\{\mathbf{A}Q\} \equiv \sum_{\mu,\nu=x,y,z} \frac{\partial^2 (A_{\mu\nu} Q)}{\partial_\mu \partial_\nu} \quad (6)$$

The anisotropic second-order derivative on the right-hand side of eq 3 arises from the anisotropic distribution of the tangent vector $\mathbf{u}$. At equilibrium, eqs 4 and 5 follow Gaussian chain statistics, and hence the usual SCF equation for $Q(s,\mathbf{r};s',\mathbf{r}')$ can be recovered from eq 3. However, under flow or highly nonequilibrium conditions, all the variables in the above equations including $P(\mathbf{u};s,\mathbf{r})$ and $Q(s,\mathbf{r};s',\mathbf{r}')$ are time-dependent, and we assume that the conformation distribution $Q(s,\mathbf{r};s',\mathbf{r}')$ follows the orientation distribution of the tangent vectors $\mathbf{P}(\mathbf{u};s,\mathbf{r})$ at any instance, i.e., adiabatic approximation. It is justifiable as $P(\mathbf{u};s,\mathbf{r})$ describes the slowest dynamic processes of the system, and also there is a clear time scale separation between the reptation time and the Rouse time of the segments. Here we note that these two quantities $P(\mathbf{u};s,\mathbf{r})$ and $Q(s,\mathbf{r};s',\mathbf{r}')$ can be described in a unified way by introducing a generalized two-point correlation function $\tilde{Q}(s,\mathbf{r},\mathbf{u};s',\mathbf{r}',\mathbf{u}')$ which is the statistical weight of the conformations specified by $(s,\mathbf{r},\mathbf{u})$ and $(s',\mathbf{r}',\mathbf{u}')$. However, we intentionally separate the quantities $P(\mathbf{u};s,\mathbf{r})$ and $Q(s,\mathbf{r};s',\mathbf{r}')$ so that the assumptions made on these quantities become clear. In so doing, we do not lose any important information as having the information on $P(\mathbf{u};s,\mathbf{r})$, the two-point correlation function $\tilde{Q}(s,\mathbf{r},\mathbf{u};s',\mathbf{r}',\mathbf{u}')$ can be constructed by solving the path integral equation (3) under the given $\mathbf{A}(s,\mathbf{r})$, $\bar{\mathbf{u}}(s,\mathbf{r})$, and $V(\mathbf{r})$. We can therefore retain all the necessary information.

In eq 3, the external potential field $V(\mathbf{r})$ should be determined in such a way that the segment density distribution calculated using $Q(s,\mathbf{r};s',\mathbf{r}')$ fits the incompressible condition and the segment density profile assumed in the potential field $V(\mathbf{r})$. Because of this reason, $V(\mathbf{r})$ is called a self-consistent field.[5−12] To determine $P(\mathbf{u};s,\mathbf{r})$, we have to consider the dynamical processes of the chain. In dense polymer solutions and polymer melts, the time evolution of the tangent vector distribution function $P(\mathbf{u};s,\mathbf{r})$ obeys the reptation dynamics. In the linear viscoelastic regime,[1] only the thermal diffusive motion of the chain in a tube is important. For a highly deformed polymer system, the model must account for the following dynamical processes: (1) advection of the segments due to the flow, (2) deformation of the chain due to the external flow, (3) thermal diffusion of the chain in the tube, (4) chain retraction after a large deformation, (5) biased reptation due to the inhomogeneity in the segment density, and (6) constraint release (or double reptation). Recently, several extensions of the original reptation theory by including these processes have been proposed.[18−21] Those models are constructed by taking the chain conformation and the total chain length as independent dynamical variables. We here propose a rather simpler model for $P(\mathbf{u};s,\mathbf{r})$, in which the tensor $\mathbf{A}(s,\mathbf{r})$ describes both the chain conformation and the total chain length simultaneously.

The time evolution of $P(\mathbf{u};s,\mathbf{r})$ is driven by the dynamical processes 1−6 listed above. Let us assume that the flow velocity field $\mathbf{v}(\mathbf{r})$ is externally given. (A

way of self-consistent determination of $\mathbf{v}(\mathbf{r})$ will be given later.) Under such a circumstance, the deformation of the chain is described by the velocity gradient tensor $(\nabla\mathbf{v}(\mathbf{r}))^{\mathrm{T}}$. Using this velocity gradient tensor, the time evolution of $P(\mathbf{u};s,\mathbf{r})$ is given by the following equation:

$$\frac{\partial}{\partial t}P(\mathbf{u};s,\mathbf{r}) = -\nabla\cdot[\mathbf{v}(\mathbf{r})\,P(\mathbf{u};s,\mathbf{r})] + \frac{\partial P(\mathbf{u};s,\mathbf{r})}{\partial \mathbf{u}}\cdot(\nabla\mathbf{u})^{\mathrm{T}}\cdot\mathbf{u} - \frac{\partial}{\partial s}j(\mathbf{u};s,\mathbf{r}) + \alpha(s,\mathbf{r})\int \mathrm{d}\mathbf{u}'\,[j(\mathbf{u}';0,\mathbf{r}) - j(\mathbf{u}';N,\mathbf{r})] \quad (7)$$

where we did not show the time t explicitly in the arguments of $P(\mathbf{u};s,\mathbf{r})$.

The first, second, third, and fourth terms on the right-hand side of eq 7 are the contributions from the advection, flow deformation, reptation (including chain retraction and biased reptation), and constraint release, respectively. The contribution from the flow velocity, i.e., the second term, originates from the change in the distribution of the tangent vector $\mathbf{u}$ due to the external deformation described by the velocity gradient tensor $(\nabla\mathbf{v}(\mathbf{r}))^{\mathrm{T}}$.

The third term, the flux of the reptation current $j(\mathbf{u};s,\mathbf{r})$, is the probability flux due to the sliding motion of the chain along the tube (i.e., the contour of the chain) and is explicitly given as

$$j(\mathbf{u};s,\mathbf{r}) = -D_{\mathrm{c}}\frac{\partial}{\partial s}P(\mathbf{u};s,\mathbf{r}) + w(s,\mathbf{r})\,P(\mathbf{u};s,\mathbf{r}) \quad (8)$$

where D_{c} is the one-dimensional diffusion constant of the center of mass of the chain along the tube and $w(s,\mathbf{r})$ is the drift velocity of the sth segment at position $\mathbf{r}$ along the tube. This drift velocity is composed of two contributions. One is the retraction of the elongated chain in the tube. As the end-to-end distance of a deformed segment is proportional to $\sqrt{\mathrm{tr}\mathbf{A}(s,\mathbf{r})}$, the drift velocity of the sth segment is proportional to the gradient of this local extension of the segment. The other contribution to $w(s,\mathbf{r})$ is the biased reptation caused by the spatial inhomogeneity in the self-consistent field $V(\mathbf{r})$. This biased reptation mimics the chain motion in a tube, which is driven by the gradient of the self-consistent field.[8] Combining these two contributions, we obtain the following expression for $w(s,\mathbf{r})$:

$$w(s,\mathbf{r}) = -\frac{3k_{\mathrm{B}}T}{a^3\varsigma}\frac{\partial}{\partial s}\sqrt{\mathrm{tr}\,\mathbf{A}(s,\mathbf{r})} + \frac{1}{a\varsigma}\left[\bar{\mathbf{u}}\cdot\nabla V(\mathbf{r}) + \frac{1}{2}\mathbf{A}(s,\mathbf{r}):\nabla\nabla V(\mathbf{r})\right] \quad (9)$$

where ς is the friction constant between a segment and the tube. Here, we note that the biased reptation term (i.e., the second term in eq 9) is approximated by the first few terms in the gradient expansion of the self-consistent field $V(\mathbf{r})$. Such an approximation is consistent with the treatment of the self-consistent field in eq 3.

The last term on the right-hand side of eq 7 is the contributions from the constraint release process.[21] As an entanglement point is sustained by a pair of chains, when one of these two chains reptates out through the entanglement point, it frees a part of the other chain simultaneously. The rate of loss of the entanglements is proportional to the flux of $P(\mathbf{u};s,\mathbf{r})$ flowing out from the both chain ends. The same amount of relaxation should take place on the other chain sharing the entanglement. If the probability of finding an entanglement point at the sth segment of a chain is $\alpha(s,\mathbf{r})$, the relaxation due to the constraint release is given by the fourth term on the right-hand sides of eq 7.

Equation 7 should be supplemented by appropriate boundary conditions. Because the orientation of the tangent vector at the both ends of the chain is completely free, $P(\mathbf{u};s,\mathbf{r})$ should be the equilibrium isotropic Gaussian distribution at a free end. On the other hand, $P(\mathbf{u};s,\mathbf{r})$ should satisfy $(\partial/\partial s)P(\mathbf{u};s,\mathbf{r}) = 0$ at a grafted end because there is no flux at the grafted end. These two conditions determine the boundary conditions for eq 7.

It is worth to note that, in deriving eq 7, we used an assumption that our polymer system is incompressible, which is guaranteed by the self-consistent potential $V(\mathbf{r})$ in eq 3. Under such an assumption, we can treat the normalization constant of the probability distribution $P(\mathbf{u};s,\mathbf{r})$ to be everywhere constant. If the polymer component is compressible, the normalization constant has a spatial dependence, which produces some other unimportant terms in eq 7.

By taking the first and second moments of eq 7 with respect to $\mathbf{u}$, we obtain the time evolution equations for $\bar{\mathbf{u}}$ and $\mathbf{A}$ as follows:

$$\frac{\partial}{\partial t}\bar{\mathbf{u}}(s,\mathbf{r}) = -\nabla\cdot[\mathbf{v}(\mathbf{r})\,\bar{\mathbf{u}}(s,\mathbf{r})] + (\nabla\mathbf{v})^{\mathrm{T}}\cdot\bar{\mathbf{u}}(s,\mathbf{r}) - \frac{\partial}{\partial s}\mathbf{j}_u(s,\mathbf{r}) + \alpha(s,\mathbf{r})[\mathbf{j}_u(0,\mathbf{r}) - \mathbf{j}_u(N,\mathbf{r})] \quad (10)$$

and

$$\frac{\partial}{\partial t}\mathbf{A}(s,\mathbf{r}) = -\nabla\cdot[\mathbf{v}(\mathbf{r})\,\mathbf{A}(s,\mathbf{r})] + \{(\nabla\mathbf{v})^{\mathrm{T}}\cdot\mathbf{A}(s,\mathbf{r}) + \mathbf{A}(s,\mathbf{r})\cdot(\nabla\mathbf{v})\} - \frac{\partial}{\partial s}\mathbf{j}_A(s,\mathbf{r}) + \alpha(s,\mathbf{r})[\mathbf{j}_A(0,\mathbf{r}) - \mathbf{j}_A(N,\mathbf{r})] \quad (11)$$

Equations 10 and 11 should be supplemented by the boundary conditions

$$\bar{\mathbf{u}}(s_0,\mathbf{r}) = \mathbf{0} \text{ and } \mathbf{A}(s_0,\mathbf{r}) = \mathbf{1} \quad (\text{if } s_0 \text{ is a free end})$$
$$\partial\bar{\mathbf{u}}(s,\mathbf{r})/\partial s|_{s=s_0} = \mathbf{0} \text{ and } \partial\mathbf{A}(s,\mathbf{r})/\partial s|_{s=s_0} = \mathbf{0} \quad (\text{if } s_0 \text{ is a grafted end}) \quad (12)$$

where $\mathbf{1}$ is the unit tensor and $\mathbf{0}$ is the zero vector/tensor. The first, second, third, and fourth terms on the right-hand side of eq 10 or of eq 11 account for advection, flow deformation, reptation (including chain retraction and biased reptation), and constraint release, respectively.[18] The quantities $\mathbf{j}_u(s,\mathbf{r})$ and $\mathbf{j}_A(s,\mathbf{r})$ in the third terms on the right-hand sides of eqs 10 and 11 are fluxes of the vector $\bar{\mathbf{u}}(s,\mathbf{r})$ and the tensor $\mathbf{A}(s,\mathbf{r})$ along the tube. Their explicit expressions are respectively

$$\mathbf{j}_u(s,\mathbf{r}) = -D_{\mathrm{c}}\frac{\partial}{\partial s}\bar{\mathbf{u}}(s,\mathbf{r}) + w(s,\mathbf{r})\,\bar{\mathbf{u}}(s,\mathbf{r}) \quad (13)$$

and

$$\mathbf{j}_A(s,\mathbf{r}) = -D_{\mathrm{c}}\frac{\partial}{\partial s}\mathbf{A}(s,\mathbf{r}) + w(s,\mathbf{r})\,\mathbf{A}(s,\mathbf{r}) \quad (14)$$

Once the statistical weight $Q(s,\mathbf{r};s',\mathbf{r}')$ is calculated, the local stress $\Pi(\mathbf{r})$ is obtained via the relation[1]

$$\Pi(\mathbf{r}) = \frac{3k_BT}{a^2}\int_0^N \mathbf{A}(s,\mathbf{r})\,\mathrm{d}s - p(\mathbf{r})\mathbf{1} \tag{15}$$

where k_BT and $p(\mathbf{r})$ are the Boltzmann constant times temperature and the static pressure. Then, the time evolution of the velocity field $\mathbf{v}(\mathbf{r})$ is determined by the momentum conservation equation for the fluid. As is usual for dense polymer solutions or polymer melts, we neglect the contribution from the inertia (Stokes approximation), and we obtain

$$\rho\frac{\partial}{\partial t}\mathbf{v}(\mathbf{r},t) = \nabla\cdot\Pi(\mathbf{r},t) + \mathbf{f}(\mathbf{r},t) \tag{16}$$

where ρ is the total density of the fluid, and $\mathbf{f}(\mathbf{r},t)$ is the volume force imposed by the inhomogeneity in the segment density, such as the thermodynamic force imposed by interfaces.

Equation 3 and eqs 10−16 form a closed set of time evolution equations. In this formulation, the complex non-Markovian character of the viscoelasticity originates from the memory of the flow history in the form of a deformed chain conformations described by the quantities $\bar{\mathbf{u}}(s,\mathbf{r})$ and $\mathbf{A}(s,\mathbf{r})$. Note that our formulation can be applied to nonlinear viscoelasticity where the chain is strongly and inhomogeneously deformed. Therefore, our formulation can predict nonlinear viscoelastic properties of polymer solutions and polymer melts based on the architectures of the constituent polymer chains.

3. Simulations

To check the validity of our model, we conducted several computer simulations on viscoelastic properties of dense polymer systems using the evolution equations presented in the previous section. As a first step of our approach, we consider a simpler situation by neglecting the terms containing $\bar{\mathbf{u}}$. Such a neglecting of $\bar{\mathbf{u}}$ terms is justified for nongrafted homopolymer melts because such a homopolymer chain is symmetric with respect to an exchange between its two ends. Although such a neglecting of $\bar{\mathbf{u}}$ terms is no longer valid for a grafted chain, we still use it because the most important part of the present formalism is the anisotropic distribution of the tangent vector described by the tensor $\mathbf{A}(s,\mathbf{r})$, and the $\bar{\mathbf{u}}$ terms are expected to be less important. We further simplifies the model by assuming that the velocity field $\mathbf{v}(\mathbf{r},t)$ is externally imposed rather than to be determined using eqs 15 and 16. This assumption highlights the effects of the coupling between the self-consistent-field model and the viscoelastic properties. The partial differential equations (3), (11), (12), and (14) are solved numerically using the Crank−Nicholson scheme.[22]

We have first checked that our model quantitatively reproduces the results of the nonlinear viscoelastic behavior of the reptation model for uniform polymer melts,[1] for which the SCF part of calculations does not play any role. We consider an instantaneous and uniform step shear deformation

$$\gamma_0 = \begin{pmatrix} 1 & 0 & \gamma_0 \\ 0 & 1 & 0 \\ 0 & 0 & 1 \end{pmatrix} \tag{17}$$

at $t = 0$ and observe the subsequent stress relaxation. Because of the homogeneous nature of the melt, the self-consistent field $V(\mathbf{r},t)$ is everywhere constant. In this case, the dominant processes are the deformation of the chain due to flow, thermal reptation, chain retraction, and constraint release. Because there is no biased reptation ($\nabla V(\mathbf{r},t) \equiv \mathbf{0}$), the change in the chain conformation obtained via eq 3 does not affect the time evolution of $\mathbf{A}(s,\mathbf{r})$ described by eqs 9, 11, 12, and 14. Therefore, we have only to solve eqs 9, 11, 12, and 14 with the velocity gradient tensor $\kappa(\mathbf{r},t) \equiv (\nabla\mathbf{v})^{\mathrm{T}} = \gamma\delta(t)$.

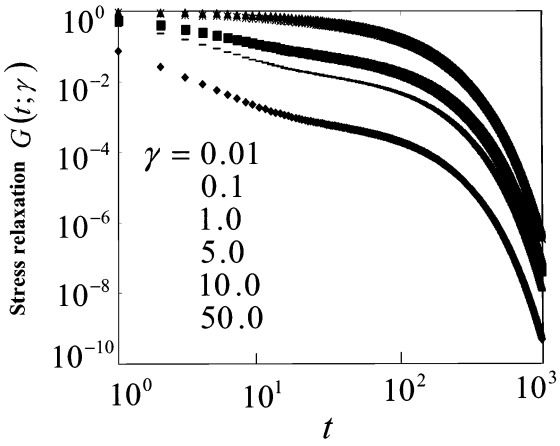

Figure 1. Stress relaxation of a uniform polymer melt after a step shear deformation is imposed at $t = 0$. From top to bottom, the magnitude of the shear deformation γ is 0.01, 0.1, 1.0, 5.0, 10.0, and 50.0, respectively.

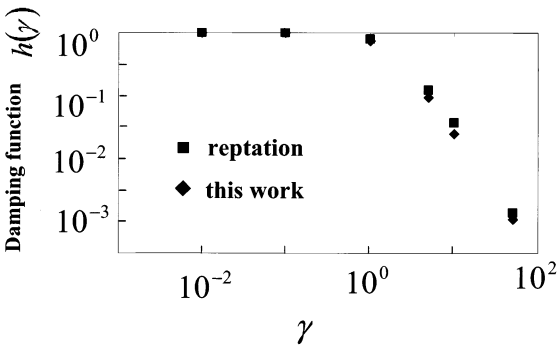

Figure 2. Comparison of the dumping function $h(\gamma)$ between our model obtained from the data in Figure 1 and the results of the reptation theory.

Simulations are performed on a melt of a homopolymer whose chain is composed of N identical segments. We assume for simplicity that the entanglement points distribute uniformly on the chain, i.e., $\alpha(s,\mathbf{r}) = 1/N$. The total chain length is taken as $N = 10.0$ in units of the tube diameter a. We set the other parameters as $a = 1.0$, $k_BT = 1.0$, $\varsigma = 1.0$, and $D_c = k_BT/N\varsigma = 0.1$. The continuous segment index s and the time t are discretized using mesh width $\Delta s = 0.1$ and $\Delta t = 0.001$, respectively.

Figure 1 shows the simulation results of the stress relaxation for various values of the shear deformation γ on double logarithmic scales. While the stress relaxation is a single exponential for small γ, it shows double step relaxation for large γ. The latter behavior is characteristic of the nonlinear viscoelastic regime. Actually, the first rapid relaxation comes from the chain retraction, and the second slow relaxation is due to the thermal reptation and constraint release.

To evaluate our model quantitatively, we calculate the dumping function $h(\gamma)$, which is defined as the amount of the initial rapid decay of the stress. In Figure 2, we compare the simulation data of $h(\gamma)$ with the theoretical

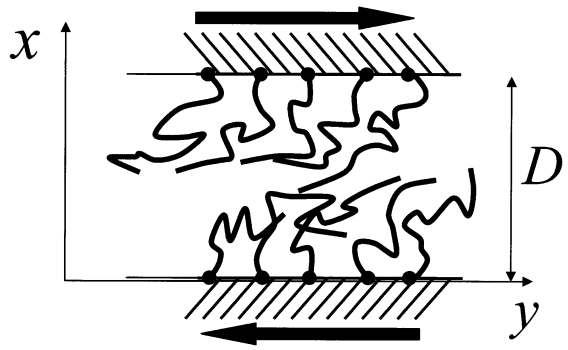

Figure 3. Schematic picture of the simulation system composed of two melt brushes.

results obtained with the reptation theory, the latter being known to give good quantitative predictions of linear polymer melts.[1] Our model quantitatively reproduces the results of the reptation theory, which means that eqs 9, 11, 12, and 14 correctly describe the relaxation of strongly deformed chain conformations in sheared uniform polymer melts. A small discrepancy between our model and the reptation theory in Figure 2 originates from the fact that the constraint release process is taken into account in the simulations while it is neglected in the reptation theory, where the constraint release process accelerates the stress relaxation.

Next, we examine the validity of our model for inhomogeneous systems. As an example, we simulate a system of two melt polymer brushes grafted on two parallel solid plates that are separated by distance D. A schematic picture of this system is shown in Figure 3. Although the segment density is everywhere constant in this case, the self-consistent field $V(\mathbf{r})$ is varying in the x-direction because of the inhomogeneous stretching of the chain due to the grafting. Therefore, the biased reptation affects the dynamics of the chains. In this example, the thermal reptation motion of the chain in the tube is negligible ($D_c = 0$) because one end of the chain is grafted to the surface. Therefore, the chain stretched by the shear deformation relaxes due to the chain retraction and the constraint release.[23]

We prepare the equilibrium state of this system and start imposing a steady shear with a shear rate κ_{xy} at $t = 0$, where x and y axes are perpendicular and parallel to the plates that are placed at $x = 0$ and $x = D$. By taking the gyration radius and the total chain length as the units of the distance and the contour length, we set $D_c = 0$, $a = 1.0$, $k_BT = 1.0$, $\varsigma = 1.0$, $N = 1.0$, and $\kappa_{xy} = 1.0$. The mesh widths $\Delta x = \Delta y = 0.1$, $\Delta t = 0.000\,001$, and $\Delta s = 0.005$ are used. In Figure 4, the temporal evolutions of the shear stress at the solid surface are shown for the cases with $D = 0.5$, 1.0, 2.0, and 4.0, respectively. We observe, in each case, that the shear stress reaches a maximum and decays monotonically. The inset figures show the single chain conformations (contour lines of the segment density) at $t = 0.0$ (left) and $t = 1.0$ (right) for the case with $D = 2.0$, from which one can confirm that the chain is strongly deformed.

In Figure 5, the time evolution of the segment density profile of the brush grafted to the surface at $x = 0$ is shown. The edge profile of the brush becomes steeper when the shear is imposed. This is due to the reduction of the overlapping between the two brushes in the central region in order to reduce the unfavorable entanglements.

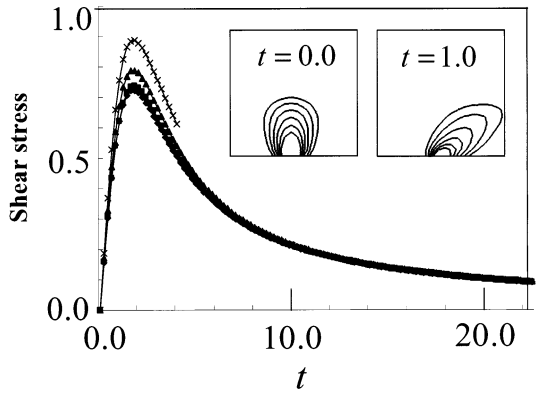

Figure 4. Temporal evolution of the shear stress at the grafting surface of a two-brush system under shear $\kappa_{xy} = 1.0$. From bottom to top, the distances between the two solid plates are taken to be $D = 0.5$, 1.0, 2.0, and 4.0, respectively. The inset figures are the contour line representations of the segment density distributions of a single chain at $t = 0.0$ (left) and $t = 1.0$ (right) for the case with $D = 2.0$.

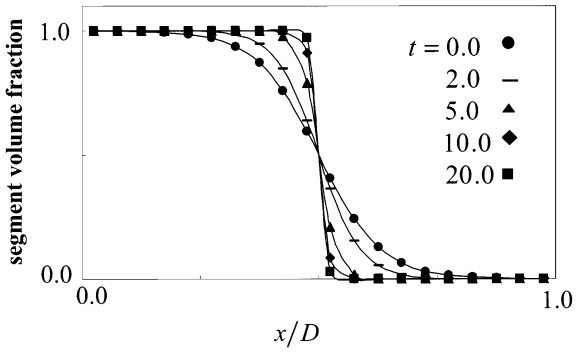

Figure 5. Time evolutions of the segment density profiles of the brush grafted on the surface at $x = 0$ of the same simulation as Figure 4 with $D = 2.0$ are shown for $t = 0.0$, 2.0, 5.0, 10.0, and 20.0, respectively.

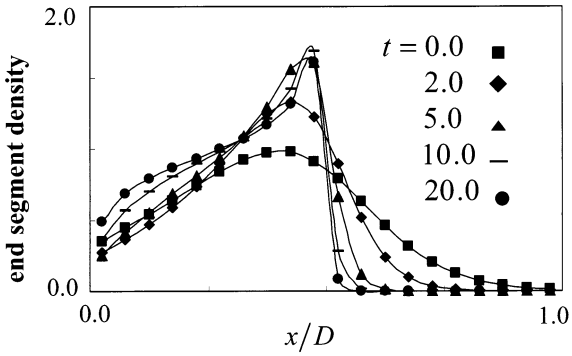

Figure 6. Distribution functions of the free end segments of the chains grafted to the surface at $x = 0$ of the same simulation as Figure 4 with $D = 2.0$ are shown for $t = 0.0$, 2.0, 5.0, 10.0, and 20.0, respectively.

One of the advantages of the self-consistent-field theory is that it can give detailed information on the chain conformation, such as the distribution of specific segments. In Figure 6, we show the time evolution of the distribution of the free end segments in the x direction. In the initial equilibrium state, the free ends distribute broadly between the two plates. When we shear this system, however, the free ends are accumulated at the center of the two plates, i.e., at the interface between the two brushes. This is due to the segregation of the two brushes mentioned above.

The simulation results we obtained above for the brush system are qualitatively consistent with the results of the recent Monte Carlo simulations using molecular models.[24,25] Neelov et al. conducted a Monte Carlo simulation of many chains grafted to two plates and observed the change in the segment density distribution before and after the shear is imposed.[24] They observed that the same tendency as we observed in the behavior of the distributions of the total segment and the free end segments. A similar change in the segment density is also reported by Saphiannikova et al. using a hybrid model between the self-consistent-field theory and the Brownian dynamics simulation technique.[25] Note that the usual static self-consistent-field theory based on the local equilibrium assumption cannot reproduce such a change in the brush density profile because the deformations of a Gaussian chain in x and y directions are independent, as is pointed out in ref 3.

4. Conclusions

As a conclusion, by combining the SCF and reptation theories, we have proposed a unified molecular model for inhomogeneous polymer systems. This model not only provides a unique theoretical framework in modeling homopolymer, polymer mixtures, and copolymers under strong flow conditions but also gives a systematic way to specify the boundary conditions of polymeric fluid flow at microscopic molecular level.

In this study, we treated the flow field $\mathbf{v}(\mathbf{r},t)$ as an externally imposed one. However, it should be determined by solving full hydrodynamic governing equations including eqs 15 and 16. Such full flow simulations can be done by applying fast Fourier transform[26] or other numerical techniques[27] in computational rheology. Computer simulation of our unified model including full hydrodynamic effect is underway and will be reported in our future publications.

Acknowledgment. The authors thank K. Furuichi, H. Morita, R. Hasegawa, J. D. Schieber, G. J. A. Sevink, A. V. Zvelindovsky, J. G. E. M. Fraaije, G. J. Fleer, G. H. Ko, S. Solovyov, and M. C.-Y. Huang for useful comments. T.K. thanks Y. Shnidman for sending his preprint to us prior to its publication. This work is supported by the Scientific Research Fund of the Ministry of Education, Culture, Sports, Science and Technology, Japan, and Japan Society for the Promotion of Science. T.K. thanks NWO, The Netherlands, for supporting his stay at Leiden University.

References and Notes

(1) Doi, M.; Edwards, S. F. *The Theory of Polymer Dynamics*; Oxford University Press: Oxford, 1986.
(2) Tanaka, H. *Phys. Rev. Lett.* **1996**, *76*, 787.
(3) Zurina, E. B.; Borisov, O. V.; Pryamitsyn, V. A. *J. Colloid Interface Sci.* **1990**, *137*, 495.
(4) Harden, J. L.; Cates, M. E. *Phys. Rev. E* **1996**, *53*, 3782.
(5) Fleer, G. J.; et al. *Polymers at Interfaces;* Chapman & Hall: London, 1993.
(6) Matsen, M. W.; Schick, M. *Phys. Rev. Lett.* **1994**, *72*, 2660.
(7) Fraaije, J. G. E. M. *J. Chem. Phys.* **1993**, *99*, 9202.
(8) Kawakatsu, T. *Phys. Rev.* **1997**, *E56*, 3240; *Phys. Rev.* **1998**, *E57*, 6214.
(9) Hasegawa, R.; Doi, M. *Macromolecules* **1997**, *30*, 3086.
(10) Morita, H.; Kawakatsu, T.; Doi, M. *Macromolecules* **2001**, *34*, 8777.
(11) Morita, H.; Kawakatsu, T.; Doi, M.; Yamaguchi, D.; Takenaka, M.; Hashimoto, T. *Macromolecules* **2002**, *35*, 7473.
(12) Furuichi, K.; Nonomura, C.; Kawakatsu, T.; Doi, M. *J. Chem. Phys.* **2002**, *117*, 9959.
(13) Kawakatsu, T. Presentation at the Knowledge Foundation's 2nd International Conference on "Multiscale Modelling−Bridging the Gap between Atomistic and Mesoscales, Boston, 2001.
(14) Kawakatsu, T. Presentation at the International Conference on Chain Molecules at Interfaces−SCF Theory and Experiments, Wageningen, 2002.
(15) Maurits, N. M.; Zvelindovsky, A. V.; Fraaije, J. G. E. M. *J. Chem. Phys.* **1998**, *109*, 11032.
(16) Fredrickson, G. H. *J. Chem. Phys.* **2002**, *117*, 6810.
(17) Mihajlovic, M.; Lo, T. S.; Shnidman, Y. *Macromolecules*, submitted.
(18) Hua, C. C.; Schieber, J. D. *J. Chem. Phys.* **1998**, *109*, 10018.
(19) Mead, D. W.; Larson, R. G.; Doi, M. *Macromolecules* **1998**, *31*, 7895.
(20) Milner, S. T.; McLeish, T. C. B.; Likhtman, A. E. *J. Rheol.* **2001**, *45*, 539.
(21) Des Cloizeaux, J. *Europhys. Lett.* **1988**, *5*, 437.
(22) Press, W.; Teukolsky, S. A.; Vetterling, W. T.; Flannery, B. P. *Numerical Recipes in C*, 2nd ed.; Cambridge University Press: New York, 1992.
(23) Marrucci, G. *J. Non-Newtonian Fluid Mech.* **1996**, *62*, 279.
(24) Neelov, I. M.; Borisov, O. V.; Binder, K. *J. Chem. Phys.* **1998**, *108*, 6973.
(25) Saphiannikova, M. G.; Pryamitsyn, V. A.; Cosgrove, T. *Macromolecules* **1998**, *31*, 6662.
(26) Jupp, L.; Kawakatsu, T.; Yuan, X.-F. *J. Chem. Phys.* **2003**, *119*, 6361.
(27) Yuan, X.-F.; Doi, M. *Colloids Surf., A* **1998**, *144*, 305. Yuan, X.-F. *Phys. Chem. Chem. Phys.* **1999**, *1*, 2177.

MA0205257